

# Antenna-Coupled Microcavity Enhanced THz Photodetectors

D. Palaferri<sup>1</sup>, Y. Todorov<sup>1</sup>, S. Barbieri<sup>1</sup>, D. Gacemi<sup>1</sup>, Y.N. Chen<sup>1</sup>, A. Vasanelli<sup>1</sup>, L. H. Li<sup>2</sup>,

A. G. Davies<sup>2</sup>, E. H. Linfield<sup>2</sup>, and C. Sirtori<sup>1</sup>

<sup>1</sup>Laboratoire Matériaux et Phénomènes Quantiques, Université Paris Diderot – CNRS UMR 7162, 75013 Paris, France

<sup>2</sup>School of Electronic and Electrical Engineering, University of Leeds, Leeds LS2 9JT, United Kingdom

**Abstract**—Plasmonic THz photodetectors have been realized in this work, by implementing the active region of a 5 THz quantum well detector with an antenna-coupled microcavity array. Our results demonstrate a clear improvement in responsivity, polarization insensitivity and background limited performance.

## I. INTRODUCTION

QUANTUM Well Infrared Photodetectors (QWIPs) have been investigated in the past 20 years as valid solution to the demand of fast and high sensitive detection in the infrared and far-infrared spectral region ( $5\mu\text{m} < \lambda < 200\mu\text{m}$ )<sup>1,2</sup>. These devices use intersubband (ISB) transitions in a semiconductor quantum well (QW) superlattice (mainly n-type doped GaAs/AlGaAs) to generate photocurrent. Recently<sup>3</sup>, we demonstrated an antenna-coupled microcavity geometry for QWIP operating at a wavelength of  $9\mu\text{m}$  which enables an improved light coupling, a reduced dark current and a higher temperature performance. Here we report on the implementation of 5 THz quantum well photodetector<sup>4</sup> exploiting a patch antenna cavity array<sup>5,6</sup>. The benefit of our plasmonic architecture on the detector performance is assessed by comparing it with detectors made using the same quantum well absorbing region, but processed into a standard  $45^\circ$  polished facet mesa<sup>4</sup>.

## II. RESULTS

Our device is based on an MBE (molecular beam epitaxy) grown structure, similar to sample v266 of Ref. [4]: 20 GaAs QWs, each with a thickness  $L_{\text{QW}} = 15.5$  nm and  $n$  doped across the central 10 nm regions with Si at a density of  $N_d = 6.0 \times 10^{16}$   $\text{cm}^{-3}$ , alternate with layers of AlGaAs (3% Al mole fraction) each with a thickness  $L_b = 70.0$  nm. At the top and the bottom of this periodic structure there are GaAs contact layers doped  $N_d = 1.0 \times 10^{18}$   $\text{cm}^{-3}$ , each having a thickness  $L_c = 100.0$  nm.

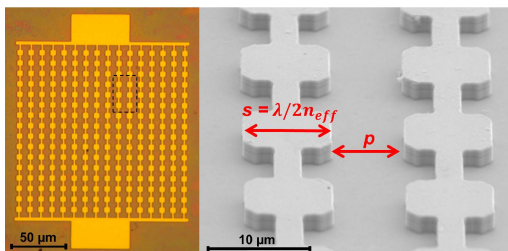


**Fig. 1.** Optical microscope (left) and scanning electron microscope (right) images of the  $9\mu\text{m}$  cavity array detector with indications of the main parameters:  $s$  is the patch size and  $p=10\mu\text{m}$  is the period length.

The patch-antenna devices shown in Figure 1 consist of a double metal structure with the top surface patterned into array

of square resonant microcavities<sup>7</sup>; devices with four different patch sizes  $s$  were tested:  $6\mu\text{m}$ ,  $7\mu\text{m}$ ,  $8\mu\text{m}$  and  $9\mu\text{m}$ .

The resonant frequency  $\nu_{\text{res}}$  of the cavity is given<sup>3,5,6</sup> by  $\nu_{\text{res}} = c/2n_{\text{eff}}s$  where  $n_{\text{eff}}$  is the effective index of the  $\text{TM}_{100}/\text{TM}_{010}$  mode, slightly higher than the index of the bulk GaAs<sup>6</sup>. The spectral photo-response of the cavity array and of the  $45^\circ$  mesa detectors are shown in Figure 2(a) and 2(b).

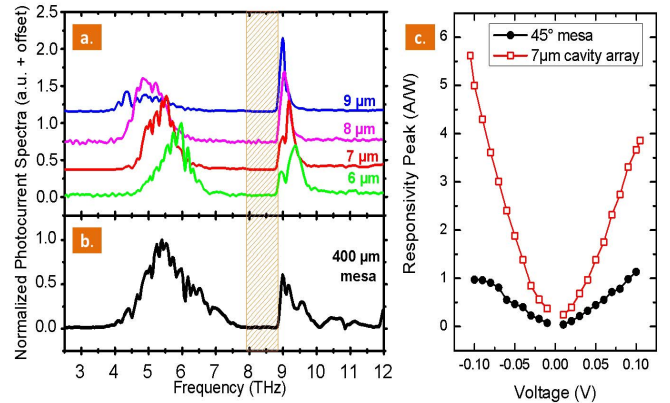


**Fig. 2.** (a) and (b) photocurrent spectra of the cavity array and of the  $45^\circ$  mesa devices, respectively; the dashed area represents the GaAs Reststrahlen band; (c) Responsivity peak vs voltage for the  $45^\circ$  mesa and the  $7\mu\text{m}$  cavity array detectors, measured with a blackbody at 500 K

The mesa device displays the typical broad shape of bound-to-quasi-continuum THz QWP, as reported in Ref. [4], with a frequency peak at 5.4 THz. The photocurrent peak for the antennas always appears at the same position as set by the cavity mode. As expected the photo-current decreases when the cavity is detuned from the maximum of the mesa photo-response at 5.4 THz. The  $s=7\mu\text{m}$  antenna device is resonant with the intrinsic photo-response, while the  $s=9\mu\text{m}$  is redshifted, resulting in cavity mode at lower energies than the intersubband absorption edge. This decreases the photo-detected signal. The plasmonic antennas couple in normal incident radiation, and collect photons over an area larger than that of the device itself, thus allowing a reduction in the dark current. Responsivity measurements were performed using a calibrated 500 K blackbody and QWIP temperature  $T = 4$  K; results are reported in Figure 2(c): the responsivity of the  $45^\circ$ -facet mesa shows values from 0 to 1 A/W in accordance with the results reported in Ref.[4]. For the  $s=7\mu\text{m}$  device, that has a cavity mode resonant with the ISB transition of the QWs, we observe a four-fold enhancement of the responsivity, with values up to 5.5 A/W in negative bias. The photoresponse is strongly enhanced due to the improved collection efficiency by the antenna effect<sup>5</sup> and reduced dark

current. This effect has a direct impact on the thermal performance of the detector, such as the BLIP (Background-Limited Infrared Performance) temperature  $T_{\text{BLIP}}$  and specific Detectivity  $D^*$ . The BLIP temperature  $T_{\text{BLIP}}$  is defined such as  $I_{\text{background}}/I_{\text{dark}} = 2$ ; under this condition the photocurrent generated by the background is exactly equal to the detector dark current<sup>1</sup>. As shown in Figure 3  $T_{\text{BLIP}} = 21$  K has been registered for the 6-7-8 $\mu\text{m}$  antennas with a field of view FOV = 54°, in comparison with the BLIP,  $T_{\text{BLIP}} = 17$  K of the mesa with a FOV=70°: the results for the antenna devices are higher than previous reported values<sup>4</sup>.

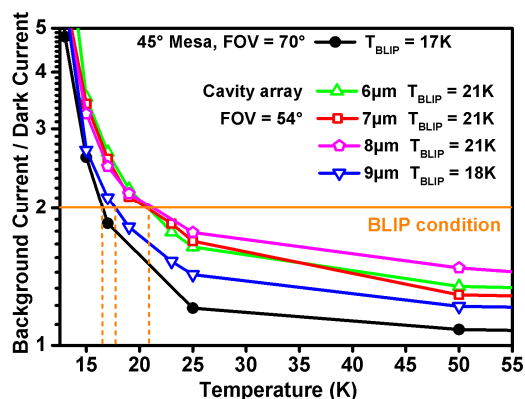


**Fig. 3.** (a) The ratio of the background and dark currents for the cavity array devices and for the 45° mesa device. The background current is  $I_{\text{background}} = I_{\text{photo}} + I_{\text{dark}}$  where  $I_{\text{photo}}$  is the photocurrent generated by a 300 K background with the indicated FOVs.

From measurements of the current-voltage characteristics and the responsivity we have also estimated the dark current-limited specific detectivity, defined as<sup>1</sup>:  $D^* = R_p A_{\text{coll}} / I_{\text{noise}}$ , where  $A_{\text{coll}}$  is the photon collection area and  $I_{\text{noise}} = (4egI_{\text{qwip}})^{0.5}$  is the current noise associated to the QWIP device, calculated knowing the photoconductive gain of the device<sup>7</sup> and the associated measured current  $I_{\text{qwip}}$ . Using photon collection areas  $A_{\text{coll}} = 1.1 \times 10^5 \mu\text{m}^2$  (mesa) and  $A_{\text{coll}} = 9.4 \times 10^4 \mu\text{m}^2$  (cavity array) we obtain maximum  $D^* = 5 \times 10^{12} \text{cmHz}^{1/2}/\text{W}$  at 4K for the arrays, in comparison with  $0.7 \times 10^{12} \text{cmHz}^{1/2}/\text{W}$  for the mesa device. We attribute this seven-fold improvement of  $D^*$  to the better photon coupling of our structure. The maximum estimated value of  $D^*$  is comparable with those of standard super-lattice detectors and of the best cryogenic cooled bolometers<sup>7,8</sup>.

Noise measurements have been carried out to confirm the detectivity estimation. Current noise spectral density have been obtained on the 9 $\mu\text{m}$  antenna detector with a setup involving a transimpedance amplifier and a spectrum analyzer, see Figure 4(left): the background current noise spectra show the typical 1/f noise (100Hz-1kHz), a plateau revealing the generation-recombination noise of the QWIP (1kHz-100kHz) and the cut-off of the amplifier (100kHz-1MHz). Figure 4 (right) shows current noise measured at 10kHz compared to the estimation from the current voltage characteristics: the good matching between measurement and estimation confirms the detectivity values that we report of the antenna-coupled devices<sup>7</sup>.

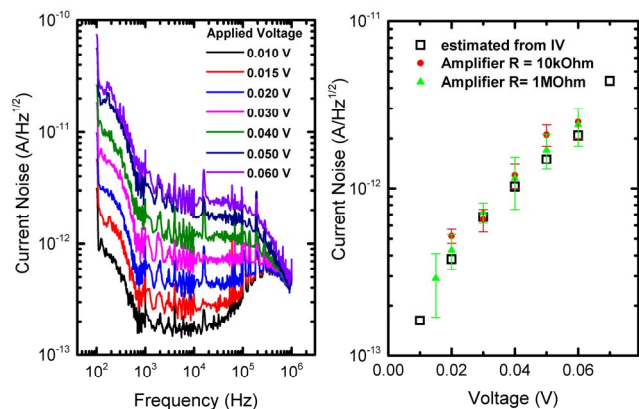


**Fig. 4.** (left) current noise spectral density measurements for the 9 $\mu\text{m}$  cavity array for different applied voltage; (right) current noise measured at 10kHz compared to the estimations from the current voltage characteristics.

### III. SUMMARY

This study shows how the concept of antenna-coupled microcavity can be applied successfully to enhance the performances of infrared and terahertz opto-electronic devices<sup>3,7</sup>. A 5 THz QWIP has been investigated and its performances have been improved in terms of its figures of merit, like responsivity, specific detectivity and BLIP temperature. Furthermore, the antenna-coupled photodetection can be still optimized by reducing the microcavity absorbing area respect to the photon collection area, while it is possible to bring the system in the critical coupling regime where all incident photons are absorbed in the structure<sup>6</sup>.

### REFERENCES

- [1] H.C. Liu, "Intersubband Transitions in Quantum Wells", edited by H. C. Liu and F. Capasso, Academic Press, San Diego, 2000.
- [2] J.C. Cao and H.C. Liu "Terahertz Semiconductor Quantum Well Photodetectors", *Semiconductors and Semimetals*, Vol. 84, 2011
- [3] Y.N. Chen, Y. Todorov, B. Askenazi, A. Vasanelli, G. Biasiol and C. Sirtori, "Antenna-coupled microcavities for enhanced infrared photodetection", *Appl. Phys. Lett.* Vol.104, 2014.
- [4] H. Luo, H.C. Liu, Song, C.Y., and Z.R Wasilewski, "Background-limited terahertz quantum-well photodetector" *Appl. Phys. Lett.* Vol.86, 2005.
- [5] Y. Todorov, L. Toso, J. Teissier, A. Andrews, P. Klang, R. Colombelli, I. Sagnes, G. Strasser, and C. Sirtori, "Optical properties of metal-dielectric-metal microcavities in the THz frequency range" *Opt. Express* Vol.18, 2010.
- [6] C. Feuillet-Palma, Y. Todorov, A. Vasanelli, and C. Sirtori, "Strong near field enhancement in THz nano-antenna arrays" *Sci. Rep.* Vol.3, (2013).
- [7] D. Palaferri, Y. Todorov, Y.N. Chen, A. Vasanelli, L. H. Li, A. G. Davies, E.H. Linfield, and C. Sirtori, "Patch antenna terahertz photodetectors" *Appl. Phys. Lett.* Vol.106, 161102 2015.
- [8] T. Ueda, Z. An, and S. Komiyama, *J. Infrared Millim. Te* 32, 5 (2010).
- [9] <http://www.terahertz.co.uk>, visited on 2/03/2015